

Instability in the propagation of fast cracks

Jay Fineberg, Steven P. Gross, M. Marder, and Harry L. Swinney

Physics Department and Center for Nonlinear Dynamics, The University of Texas, Austin, Texas 78712

(Received 12 August 1991)

We report on experimental investigations of the propagation of cracks in the brittle plastic polymethyl methacrylate (PMMA). Velocity measurements with resolution an order of magnitude better than previous experiments reveal the existence of a critical velocity (330 ± 30 m/s) at which the velocity of the crack tip begins to oscillate, the dynamics of the crack abruptly change, and a periodic pattern is formed on the crack surface. Beyond the critical point the amplitude of the oscillations depends linearly on the mean velocity of the crack. The existence of this instability may explain the failure of theoretical predictions of crack dynamics and provides a mechanism for the enhanced dissipation observed experimentally in the fracture of brittle materials.

INTRODUCTION

In the past decade the study of driven nonequilibrium systems has uncovered a rich and unexpected variety of routes by which a system can evolve from a state of relative simplicity to states of higher and higher complexity. A system driven by increasing the energy flow into it often becomes unstable to alternative modes in which the transfer of energy out of the system is enhanced. Most experiments in the field have been performed on fluids, where the instability typically results in a change of the global motion of the medium, e.g., the appearance of convection cells or Taylor rolls. Unlike fluids, the motion in a solid is constrained to small deviations from the equilibrium state. Instabilities can still occur in these materials as they are driven further from equilibrium, but the nature of these instabilities may be entirely different from those in fluids because transport must take place by means of collective modes of the material and not by global macroscopic motion. The experiments described below constitute a step toward the understanding of such instabilities.

The propagation of a crack in a brittle material under stress is a problem unfamiliar to most physicists, but it has been actively studied in the engineering community for many years. We present experimental evidence for the existence of an instability in the motion of a crack in a thin brittle plastic sheet.¹ The instability has a profound effect on the dynamics of the crack, and current theories of crack dynamics must be modified to account for it. Reinterpreting previous work,² we show that this dynamical instability results in a large increase in the energy dissipation in the medium.

The next section of this paper introduces the questions we plan to address and describes previous research. The section after that describes the experimental apparatus and methods, and the final section contains our results.

THEORETICAL AND EXPERIMENTAL BACKGROUND

A schematic representation of the system studied is shown in Fig. 1. We define the vertical direction as the z

direction. A small "seed" crack is introduced at the edge of the sample midway between the vertical boundaries of a thin plate of amorphous, brittle material. To initiate fracture, the material is then stretched by applying a uniform displacement at its vertical boundaries in slow steps until the crack starts to propagate in the x direction (see Fig. 1). We seek to describe the motion of the crack tip as a function of time as it traverses the plate.

Theoretical studies of crack motion in polymethyl methacrylate (PMMA) have occurred within two separate frameworks. The first models PMMA as a viscoelastic solid, where crack motion is limited by dissipation. Attempts to fit this model to PMMA indicate that beyond a critical velocity, on the order of 10 cm/s, viscoelastic effects become increasingly unimportant.³ Thus, to compare with our experiments in which the cracks move on the order of hundreds of meters per second, we are led to the second theoretical framework, which models PMMA as a brittle elastic solid. As a crack propagates, it creates new surface. By equating the energy flow into the crack tip with that required to create this new surface, one can derive predictions for the dynamic behavior of the crack. Most analytical progress

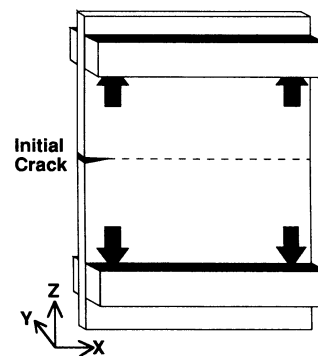


FIG. 1. Schematic representation of the method of loading used in the experiments: Stress was applied in the z direction (arrows) to the undersides of strips bonded onto the upper and lower edges of the plate. The dashed line shows the crack's direction of propagation starting from an imposed initial crack.

has been made assuming that the medium behaves according to the equations of linear elasticity. To obtain equations of motion for the crack, a determination of the fracture energy (defined as the energy needed to create crack surface per unit length) is required; the simplest assumption is that fracture energy is a material constant, independent of the propagation velocity of the crack. Predictions for the crack motion based on linear elasticity have been derived for a semi-infinite crack in an infinite two-dimensional medium by Eshelby,⁴ Kostrov,⁵ and Freund,⁶ who generalize the results of earlier work, and by Liu and Marder⁷ and Marder⁸ for the case of a crack propagating in a strip of finite width. If the change of fracture energy with velocity is not too large, all of these theories predict that the crack should smoothly and continuously accelerate until arriving at a limiting velocity given by the Rayleigh wave speed—the velocity at which waves propagate along a free surface of an elastic solid.⁹

Experiments, however, in a variety of amorphous brittle materials (glass, homolite 100, PMMA) (Ref. 10) do not confirm this picture. The observed terminal propagation speed of cracks typically approaches less than half of the predicted limiting velocity. The theories predict more than just the terminal velocity, but there has been remarkably little experimental effort to confirm the results of dynamical theories in detail. The most detailed comparison of theory and experiment was done by Bergkvist on PMMA.¹¹ Using empirical values for the effective velocity dependence of the fracture energy,¹² Bergkvist showed in highly detailed crack-arrest experiments at low velocities (less than 200 m/s or $0.21V_R$, where V_R is the Rayleigh wave speed, which is 926 m/s in PMMA) that cracks travel in accordance with predictions based on linear elastic theory to within about 10%. For higher crack velocities, experiments of this detail and accuracy have not been performed. Once speeds approach about 30% of V_R , theory and experiment are often compared by “adjusting” the theory, so that, for example, the limiting velocity in the theory is taken to be the measured terminal crack velocity.¹³ The discrepancy between theory and experiment can be accounted for by invoking sufficient “dissipation,”^{13,14} but quantitative attempts to evaluate the amounts of dissipation show it to be far too small to explain the observed “sluggishness” of the crack.³ The discrepancies between theory and experiment indicate that there indeed exist significant gaps in our understanding of these basic fracture processes.

In all of these calculations, the crack is assumed to move along a straight line, certainly a possible motion, but not necessarily a stable one. The surface created by the crack, however, is not necessarily smooth and flat as assumed in the theoretical treatments. In brittle materials such as glass or brittle plastics, a characteristic pattern called¹⁵ “mirror, mist, hackle” appears along the fracture surface. The “mirror” or macroscopically smooth surface appears as fracture initiates. As the crack progresses, this featureless region evolves into the “mist” region, where, although the surface is still relatively smooth, it appears misty or diffuse to the eye. As the crack progresses still further, the surface becomes

progressively rougher until, in the rough “hackle” regime, surface structure is in evidence on many scales. A closer look at the “mist” and “hackle” regions in brittle acrylics such as PMMA has revealed² a well-defined, roughly periodic riblike structure along the fracture surface. The period of this structure¹⁶ is on the order of a millimeter, although PMMA is entirely amorphous on that scale. Thus the theoretical assumption that cracks travel along perfect straight lines is questionable except possibly in the initial “mirror” region. The reasons for the existence of the surface structure are not understood and the motivation for our experiments was, in part, the desire to determine whether an oscillating mode of the crack tip might be responsible for controlling crack motion after some critical velocity.

EXPERIMENTAL SYSTEM AND METHODS

To enable comparison with two-dimensional elastic theory, our experiments were performed on thin (1.6- and 3.2-mm-thick) sheets of PMMA. The samples had dimensions in the direction of applied stress (z or “vertical” direction) of 14–25 cm and ranged from 10 to 20 cm in the direction of crack propagation (x direction). Experiments were conducted on PMMA made by different processes (extruded and cell cast) and by different manufacturers (Cyro, Rohm and Haas, Dupont, and KSH). A sketch of a prepared sample is shown in Fig. 1. Each sample was first machined to ensure that the sides were parallel to better than 0.02 mm. Machined rectangular strips were then bonded onto the sheet with PMMA solvent to form steps at the top and bottom boundaries of the sample that were parallel to within 0.02 mm. These strips uniformly transferred the applied stress to the sample.

The sample boundaries were strained by means of a computer-controlled tensile testing device. The device consisted of two translating “grips” made to fit against the undersides of the strips bonded onto the top and bottom edges of the sample. The grips were mounted on parallel rails so that they were constrained to travel in the z direction and were moved apart by means of a stepping motor. The rate of boundary displacement could be varied between 0 and 150 mm/min in displacement increments of 0.1 μm . The applied stress was measured by means of a load cell whose output was continuously monitored at 25 kHz and stored in the computer; stresses of 0–25 000 N could be measured with a resolution of 10 N. Since we were interested in measuring signal levels down to about 1 μV , the entire apparatus was encased in a copper box for shielding purposes.

The location of the crack tip as a function of time was determined from measurements of the resistance of a thin (35–40-nm) uniform layer of aluminum evaporated onto one face of the sample.¹⁷ As a crack progresses through the sample, the stressed material behind the tip relaxes, tearing the aluminum layer adhered to it and thereby changing the resistance of the sample. The dependence of the crack length on the sample resistance was calculated numerically for the appropriate geometry of the plate. The validity of this calibration was checked carefully by direct measurements of the resistance of plates with sta-

tionary cracks.

The resistance of the layer as a function of time was measured by means of the apparatus shown in Fig. 2. The aluminum layer (typically having an initial resistance on the order of 1Ω) was one resistance leg of a Wheatstone bridge whose output was amplified and then digitized at 12 bits at a rate of 10 MHz. In order to capture the entire length of the crack at high spatial resolution, two digitizing channels were cascaded, each with a different gain and offset, so that each channel was triggered as the previous one exhausted its range. An order-of-magnitude change in the sample's resistance (corresponding to approximately the first 75% of its width) was typically monitored over the course of an experiment. Thus the crack length for discretely spaced times was obtained. The crack velocity was determined by dividing the distances corresponding to each discrete jump in the digitized voltage by the elapsed time since the previously measured voltage change.

The Wheatstone bridge was powered by a 3-V battery to reduce noise and maintain a constant excitation voltage. The bridge configuration was used to obtain a bipolar output voltage, which was amplified to enable us to exploit fully the $\pm 1.25\text{-V}$ input range of our analog-to-digital converters (Burr-Brown model ZPD 1002). The amount of amplification needed to saturate this input range varied in the range 7–300, depending on both the location of the crack in the sample and the desired spatial resolution. To resolve fully the dynamics of the crack, we maintained a minimum bandwidth of 2.5 MHz and limited the rms measurement noise to a maximum level of $\frac{1}{2}$ bit. The noise in the system came from three sources: external pickup, intrinsic noise due to the Johnson noise of the bridge, and intrinsic noise in the electronics. The pickup noise was reduced by careful attention to system grounds, heavy shielding of both the tensile testing apparatus and all low-level lines, and using batteries (12 V) to supply power to the electronics. We reduced the Johnson noise by keeping the size of all resistors in the input stage of the electronics to a minimum and by using ultralow-noise components. The operational amplifiers used were Texas Instruments LT1028, which have a minimum unity gain bandwidth of 50 MHz and an equivalent input noise of $1 \text{ nV}/(\text{Hz})^{1/2}$. At high gain, the noise level attained was at the intrinsic noise limit.

These measurements yielded crack velocities with a

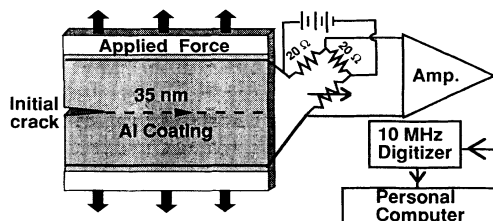


FIG. 2. This schematic representation of the experimental apparatus indicates how resistance measurements are performed to determine the location and velocity of a crack tip. The dashed line indicates the path of the crack.

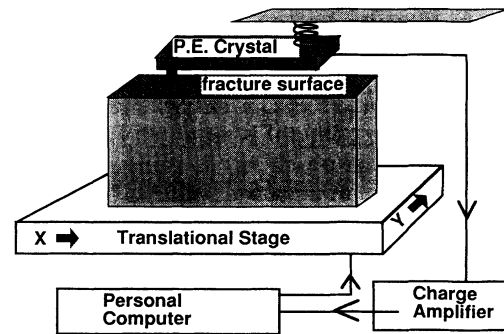


FIG. 3. Schematic diagram of the profilometer used to determine the surface profile of a crack surface. A piezoelectric crystal (P.E.) was used as its sensor.

resolution of 30 m/s and a spatial resolution of between 0.005 and 0.1 mm. These results are an order-of-magnitude more precise in both temporal and spatial resolution than previous results obtained by nonintrusive methods.¹⁸

The experimental procedure was as follows. A small crack between 3 and 5 mm in length was made midway between the grips ($z=0$), starting at the edge of the sample ($x=0$). This seed crack, from which fracture would initiate, was created either a razor blade edge or by melting through the plastic with a heated brass shim of approximately 0.1 mm in width. By varying the length and sharpness of the initial crack tip, the level of stress needed to initiate fracture (and therefore the eventual initial acceleration of the crack) could be controlled.

After making the initial crack, stress was applied at about half of the critical value needed for the initiation of fracture. From that point, the strain was then increased every 10–20 s by a fixed displacement δL (typically $\delta L/L \sim 1 \times 10^{-4}$, with L the vertical length of the sample), until the sample broke. The rate of strain was chosen so as to have at most one 0.1- μm displacement step occur within the typical duration time of fracture (about 300–400 μs), thereby eliminating elastic waves induced by the loading of the sample.

The profile of the fracture surface after fracture was measured by means of an x - y scanning profilometer, as shown in Fig. 3. The sensor of the device is a piezoelectric crystal, which is sandwiched between a stylus and a leaf spring. The stylus is deflected as the sample is translated horizontally by a computer-controlled translational stage. The output of the crystal is fed into a charge amplifier whose output is digitized at 12 bits and stored in the computer. The resolution in the xy direction is 25 μm and is limited by the radius of the stylus. Deflections of the stylus over a range of 0–1 mm normal to the crack surface are measured with a resolution of 0.1 μm .

RESULTS

Fracture surface profiles and velocity measurements taken together provide convincing evidence for a dynamical instability of cracks in PMMA. A typical fracture

surface profile, composed of 30 profilometer scans in the x direction spaced 0.05 mm apart in the y (transverse) direction, is shown in Fig. 4. The surface is initially featureless on scales larger than 1 μm . Suddenly a jagged structure appears and subsequently develops into coherent oscillations with a wavelength on the order of 1 mm in the direction of the propagation of the crack. This wavelength is unchanged when the plate thickness is increased from 1.6 to 3.2 mm or if the length of the plate in the z direction is increased from 14 to 25 cm.¹⁹ Past experiments have shown^{16,20} that the period of the pattern is an increasing function of the molecular weight of the monomers used to fabricate the PMMA. Since PMMA is completely amorphous on the scale of a millimeter,²¹ the source of these oscillations is not related in any obvious way to the material structure.

The surface pattern cannot be described purely by a one-dimensional crack front. The oscillations, as can be seen in the Fig. 4, do not initially extend across the entire width of the fracture surface, but are rather well localized. In fact, in some cases more than a single oscillatory "threadlike" pattern is observed at onset. These "threads" coalesce downstream and eventually broaden to extend over the entire width of the sample.

The appearance of surface structure coincides with a marked change in the dynamical behavior of the crack, as Fig. 5 illustrates. The crack initially accelerates rapidly in the region where the fracture surface is smooth (the "mirror" region). Then, at a well-defined critical velocity V_c (indicated by the arrow in the figure), the mean ac-

celeration slows sharply and the velocity begins to oscillate.²² The emergence of these oscillations in the velocity coincides with the first jagged structure observed on the fracture surface (see Fig. 4). There is a high degree of correlation between the velocity oscillations and the observed structure on the fracture surface, as illustrated in Fig. 6. Finally, in Fig. 7 we show velocity measurements of two samples that were broken at different levels of stress.

In order to understand the velocity data, it is necessary to compare with some theory. Unfortunately, no theory has been developed for a finite-length crack in a semi-infinite plate, the simplest setting containing the basic physics of our experiment at early times. Therefore, we make use of results for a semi-infinite crack in an infinite plate, which are clearly explained in Ref. 23. For a crack of initial length l_0 and extension l , we find that the velocity V of the crack should be described by²³

$$V = V_R (1 - l_0/l), \quad (1)$$

where V_R is the Rayleigh wave speed. Although the forms for the potential and kinetic energies used to derive Eq. (1) break down as the crack speed approaches V_R , the theory continues to behave sensibly and correctly approaches the limiting velocity. In the one case where it can be checked carefully, for a semi-infinite crack in an infinite plate loaded on the crack faces, it is amazingly accurate and corresponds within 1% to the velocity predicted by Freund's theory.²³ Thus, in the early stages of

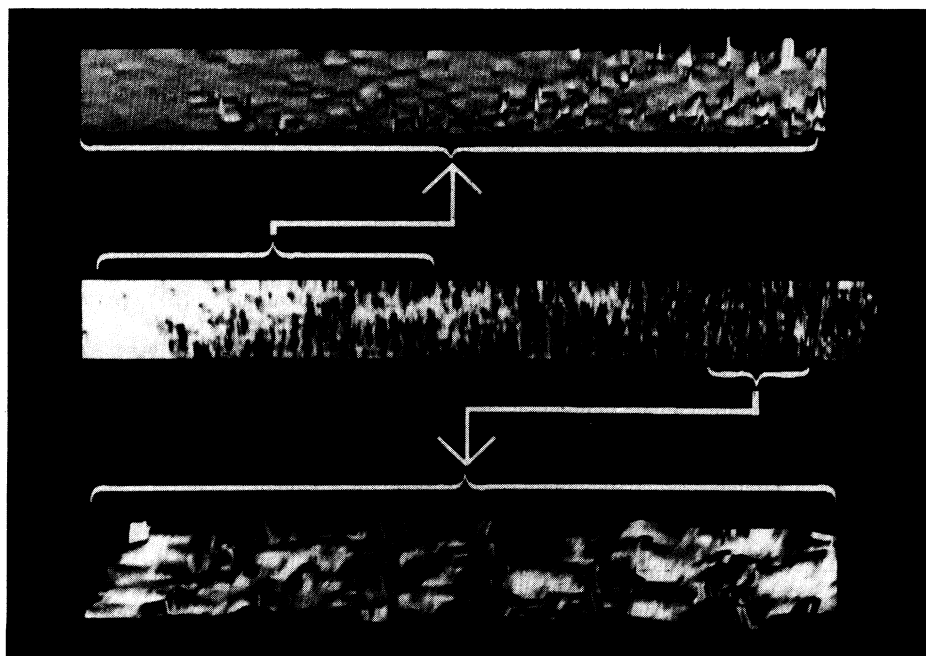


FIG. 4. Computer visualizations of the profilometer data for a crack that propagated from left to right. The central image shows an overview of a portion of the fracture surface, 62 mm \times 1.5 mm. Lighting models are used, so that the image is nearly identical to illuminated photographs of the surface. Note the ripple pattern with wavelength on the order of 1 mm. Two subregions have been magnified and shown in perspective. The onset of the instability appears in the upper image; the highest peaks are about 20 μm . The lower image contains a magnified view of the ripples created by the instability once it develops more fully; the highest peaks are about 50 μm .

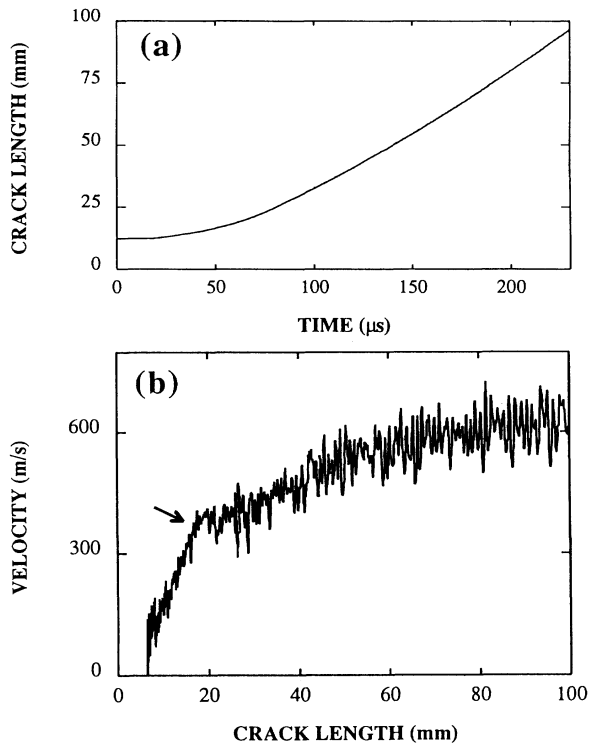


FIG. 5. (a) Length of a crack as a function of time, determined from measurements of the resistance of the thin aluminum coating on the PMMA. (b) Velocity of the crack tip deduced from the measurements shown in (a). At the critical velocity of 330 ± 30 m/s, indicated by the arrow, the mean acceleration of a crack slows, and the velocity begins to oscillate. These oscillations are much larger than the resolution.

crack propagation, Eq. (1) (upper curve in Fig. 7) should provide a good description of the crack motion. However, both the sharp break in the experimental curves at V_c and the appearance of velocity oscillations indicate a different physical behavior. This transition precedes the

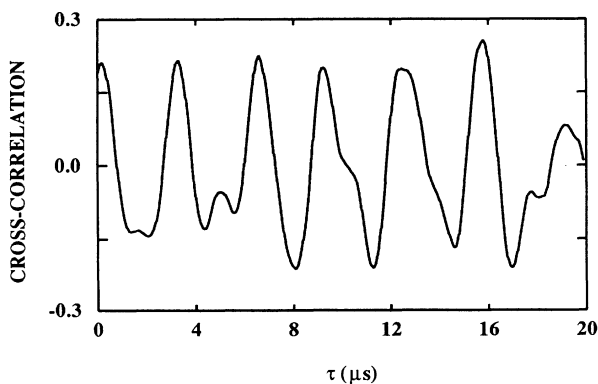


FIG. 6. Correlation of the velocity oscillations with the surface profile in a region 20 mm after transition is shown in this graph of the cross-correlation function $\Sigma_i A(t + \tau)V(t)$, where $A(t)$ and $V(t)$ are, respectively, the surface height and fluctuating part of the velocity, normalized by their rms values, and τ is the delay time.

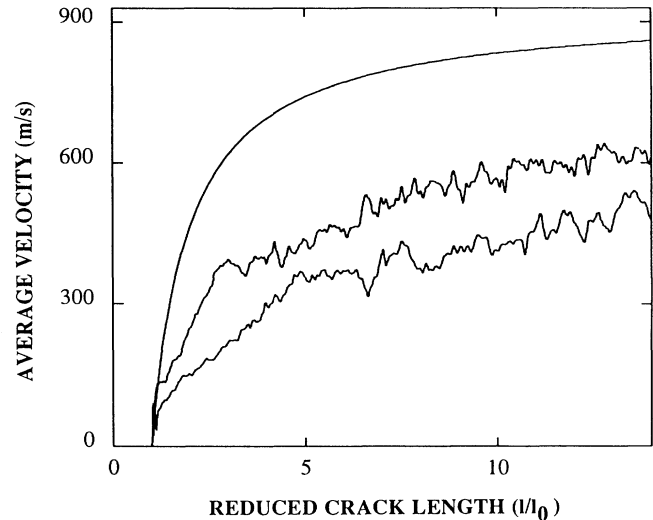


FIG. 7. Velocity as a function of crack length l normalized by the initial crack length l_0 for two different experimental runs is compared with the theory of Freund (Ref. 6) (upper curve). The initial acceleration rates depended on the sharpness of the initially imposed crack tip. The applied stress in the lower (upper) data set was 10.26 MPa (11.18 MPa). To emphasize the mean dynamics, the velocity was averaged over 1 mm in the x direction. The initial crack length l_0 was 5.3 mm for the lower curve and 6.5 mm for the upper curve.

arrival at the crack tip of the transverse and longitudinal elastic waves generated at the onset of fracture and reflected from the boundaries.²⁴ Thus the transition seems to be due to an intrinsic instability not incorporated in the present theories.

As can be seen in Figs. 5 and 7, the velocity of the crack accelerates very sharply at the onset of fracture to a velocity on the order of 100 m/s. Previous authors have considered the jump in velocity to be discontinuous.²⁵ However, our high-resolution measurements such as those shown in Fig. 8 indicate that the initial acceleration is very large (approaching 10^8 m/s²) but finite. Thus the velocity change is *continuous*. A possible reason for the large acceleration is that, prior to the onset of frac-

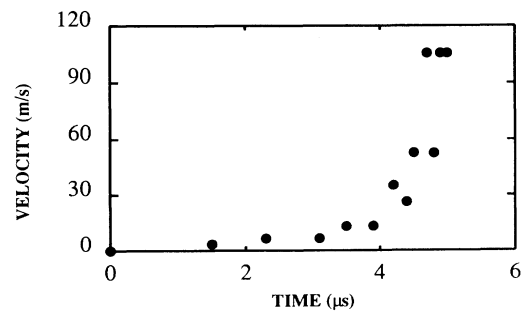


FIG. 8. Velocity of the crack as a function of time during the first 5 μ s (0.1 mm) of fracture. The data were measured on a sample having an initial crack length of 67 mm, which was 34% of the initial sample size in the x direction. The initial motion is seen to result from smooth acceleration from rest and not by a discontinuous jump to a finite velocity.

ture, the amount of energy stored in the material is larger than the minimum amount of energy necessary to sustain fracture. This could be due either to the existence of an initial crack tip that is not perfectly “sharp” (thereby blunting the singularity of the stress field at the crack tip) or to a difference in the amount of energy needed to create new surface for static and moving cracks.

Although the spatial patterns formed on the crack surface appear regular, the wavelength of the oscillations is in fact increasing. Figure 9 shows that it is the *frequency* of the oscillations rather than the wavelength that is constant. To determine the value of the critical velocity V_c , we first had to define the onset of the instability. This was determined in the following way. The fracture surface was subdivided into rectangular sections 1 mm (in the x direction) by the sheet width (1.6 or 3.2 mm in the y direction). The average surface profile $P(x)$ was defined as the average of all of the surface amplitudes greater than the local rms value of the surface profile data in each rectangle. $P(x)$ was defined in this way because, as can be seen in Fig. 4, the initial oscillations are localized in both the x and y directions and take up only a small percentage of the width of the sample. To detect the initial appearance of the oscillations, $P(x)$ must be sensitive to this. In the smooth (“mirror”) region, $P(x)$ is nearly constant and of low amplitude (on the order of $0.1 \mu\text{m}$). The onset of the instability is defined as the point x_0 where $P(x) > 3P(0)$. V_c is defined²⁶ as the velocity of the crack at x_0 . The critical velocity defined in this way slightly precedes the sharp break in the crack acceleration (see Figs. 5 and 7). This observation suggests that the instability needs to develop to a finite amplitude in order to influence measurably the dynamical behavior of the system.

The value of V_c was independent of sample geometry, sample thickness, applied stress, surrounding atmosphere, and acceleration rate of the crack. The history of

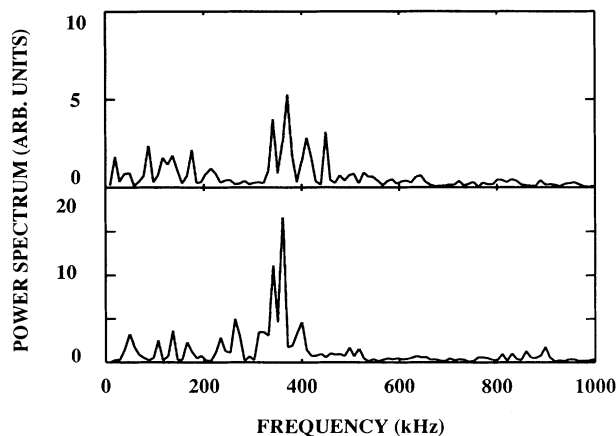


FIG. 9. Power spectra of surface height (see Ref. 30). The upper spectrum was obtained for the surface created in the $100 \mu\text{s}$ immediately following the onset of oscillations, the lower for the surface created in the subsequent $100 \mu\text{s}$. Although the mean velocity of the crack increases by over 60%, the frequency of oscillation remains constant.

how the crack arrives at V_c was wholly unimportant—whenever the crack passed the critical velocity of 330 m/s ($0.34V_R$) with a standard deviation of 20 m/s, oscillations developed. The converse was also true: Fracture surfaces that showed no pattern always had crack velocities below the critical value.

The data in Fig. 10 demonstrate that V_c is independent of the crack length at the onset of the oscillations. This indicates that V_c is not influenced by effects such as the interaction of the crack with sound waves induced by the fracture initiation and subsequently reflected back by the sample boundaries. The data were obtained in both cell-cast and extruded PMMA samples of thickness 1.6 and 3.2 mm, ranging in size from 10×25 to $20 \times 25 \text{ cm}^2$. The initial acceleration rates of the cracks in the various runs ranged from 1×10^6 to $1 \times 10^7 \text{ m/s}^2$, and the applied stress per unit area required for fracture ranged from 4.8 to 17 MPa.

To examine the effect of the surrounding medium on both the existence of the instability and value of V_c , experiments were conducted in atmospheres of air, nitrogen, and helium. Since the observed value of V_c is comparable to the speed of sound in both air and nitrogen (345 m/s at the experimental conditions of 25°C and 70% humidity), we were curious whether a “cavitation” type effect existed when the sound barrier was broken by the crack. In contrast, the sound speed in helium (965 m/s) is well above the velocities reached in PMMA and therefore should provide a good control with which to evaluate the results in air and nitrogen. Figure 11 presents a comparison of typical velocity measurements conducted in air and helium. Experiments conducted in air and nitrogen gas yielded sharp velocity spikes that approached 2000 m/s, followed by a momentary deceleration of the crack. Sharp spikes in the velocity were not observed for velocities below 300 m/s in either air or nitrogen and were not observed at all in helium. However, we did observe, as indicated in Fig. 11, small disturbances in helium that were due to the interaction of the crack with the longitudinal and transverse elastic waves generated at the fracture onset and reflected back from the

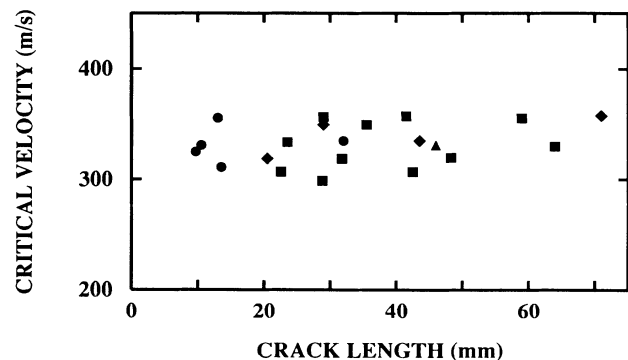


FIG. 10. Critical velocity as a function of crack length at the time of transition: circles, 1.6 mm extruded PMMA in air; squares, 3.2 mm cell-cast PMMA in air; diamonds, 3.2 mm cell-cast PMMA in helium; triangle, 3.2 mm cell-cast PMMA in nitrogen. All measurements were made at room temperature.

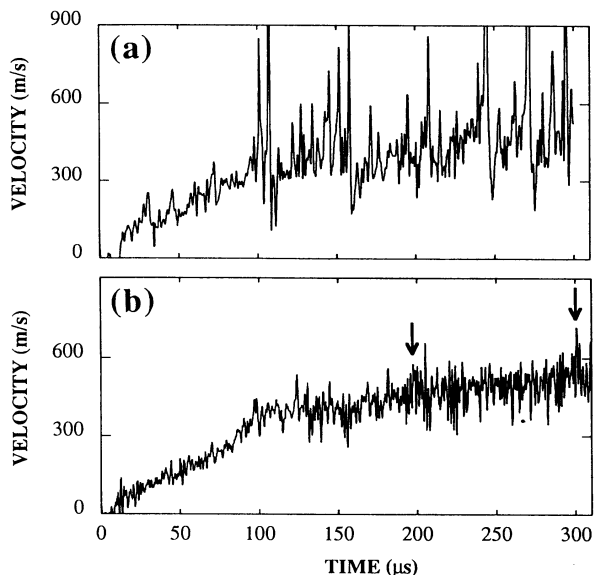


FIG. 11. Typical velocity measurements obtained in (a) air and (b) helium atmospheres. Note the absence of sharp spikes in the data in (b). The peaks at arrival times 190 and 297 μ s (indicated by arrows) correspond to velocities of 1751 and 999 m/s for reflected waves from the far boundaries in the x direction. The velocities are in excellent accord with the velocities of longitudinal and transverse waves in a thin plate, 1778 and 1013 m/s, respectively, which were determined independently from our measurements of the Young's modulus (3.3×10^{10} dyn/cm²) and of Poisson's ratio, 0.357 (Ref. 31).

far boundary in the x direction. Thus it appears that cavitation effects do indeed occur in the material as the crack speed surpasses the speed of sound in the surrounding medium. Nonetheless, the character of the instability and value of V_c were independent of the surrounding medium (see Fig. 10).

Measurements of the energy flow into the crack tip by Green and Pratt² showed a very sharp rise of the energy flow at a velocity of slightly under 400 m/s. Given the resolution of their velocity measurements, this energy increase is consistent with the onset of the instability at V_c .

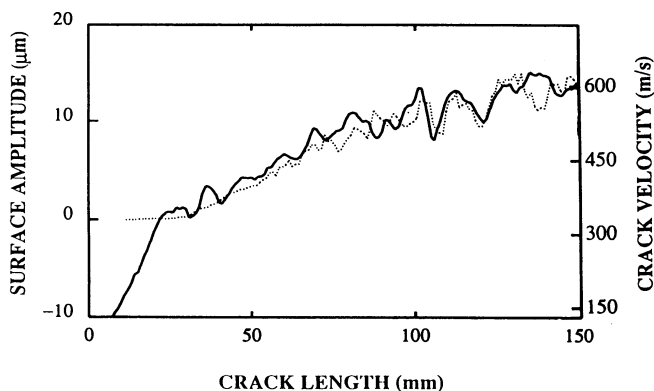


FIG. 12. Mean velocity (solid line) and rms amplitude of the fracture surface (dotted line) as a function of crack length. Note the good correspondence of even the details of the two measurements.

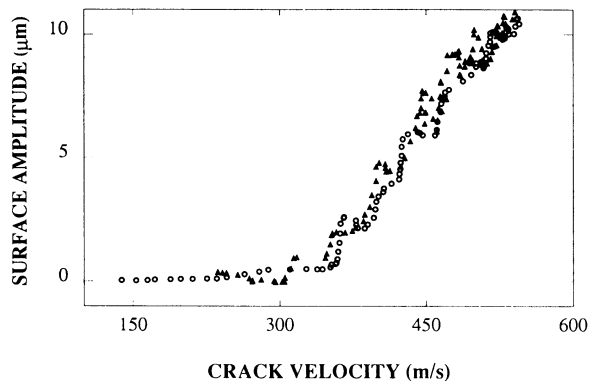


FIG. 13. rms surface amplitude as a function of mean crack velocity for two runs having initial acceleration rates differing by 30%. Note the sharpness of the transition and the linear dependence of the fracture surface amplitude on the velocity. Linear fits of the velocity data to the amplitude data in the region after the transition yield values for V_c of 324 m/s (triangles) and 333 m/s (circles), in excellent agreement with the mean value of $V_c = 330$ m/s obtained by the amplitude-threshold method described in the text.

and probably coincides with the corresponding sharp drop in the acceleration that we observe.

The mean velocity and rms surface amplitude as function of the crack length are compared in Fig. 12. For $V < V_c$ the amplitude is essentially zero, but above criticality the surface amplitude grows smoothly from zero, while the mean acceleration of the crack slows sharply.

Figure 13 shows that the surface amplitude varies linearly (within experimental resolution) with the mean velocity and can be well fitted by the function $A = 20(V - V_c)$, where A is the surface amplitude in μ m and V the crack velocity in m/s. Note the sharpness of the transition. In bifurcation theory the linear depen-

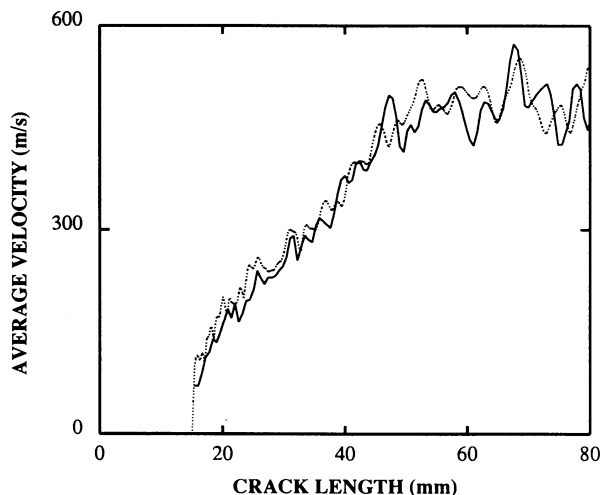


FIG. 14. Comparison of the mean velocity for two runs where the applied stress needed to precipitate fracture differed by less than 5%. The figure demonstrates the reproducibility achieved in the measurements.

dence of A on $V - V_c$ would indicate a transcritical bifurcation, which is not possible for a bifurcation to an oscillatory state.²⁷ The generic transition to an oscillatory state is by way of a Hopf bifurcation where the amplitude of the state is proportional to the square root of the distance from the bifurcation (control) parameter. Our data are not consistent with this generic scenario.

Our results were remarkably reproducible: Figure 14 shows the measured velocities of two data sets for which the applied critical stresses for fracture differed by less than 5%. This degree of reproducibility in the value of the critical stress required accurately reproducible boundary conditions, loading history, and both the size and shape of the initial crack. High reproducibility is crucial if random factors such as the existence and distribution of defects (microcracks) are to be distinguished from deterministic chaotic dynamics. The degree to which the surface structure is reproducible is a question currently under study.

CONCLUSIONS

Our high spatial and temporal resolution reveals a well-defined transition marked by the appearance of oscillations in the crack tip velocity for rapidly propagating cracks in PMMA. These oscillations are highly correlated with the fracture surface profile. This dynamical instability in PMMA occurs when the propagation velocity of a crack exceeds a critical velocity of 330 ± 25 m/s. Prior to the transition, the crack accelerates rapidly and the fracture surface is smooth and, to a large degree, featureless. The onset of the instability has a profound effect on both the pattern on the fracture surface and more importantly on the dynamics of the crack itself. The importance of this effect to the understanding of the behavior of dynamic cracks can be seen from the sharp drop in the initial rapid acceleration of the crack at the first appearance of the oscillations. The large increase in the flow of energy to the crack tip at approximately 400 m/s, as observed by Green and Pratt,² also coincides with the onset

of the instability. Thus the instability observed here could provide a major mechanism for the dissipation of energy as the system is driven further and further from equilibrium. Any theory that purports to describe the process of fracture in this (and probably other) brittle material must take the instability into account.

No mechanism for the occurrence of the observed oscillations is known, and no theory describes or predicts them, but we suspect that the basic framework within which to look for the theory is two-dimensional linear elasticity. However, elastic theory does not naturally provide the time scale of approximately $3 \mu\text{s}$ corresponding to the observed oscillations. This scale may be a reflection of a much smaller time scale somehow magnified by dynamical processes. We also mention that there is some precedent for the study of dynamical instabilities in two-dimensional linear elasticity. An analysis by Yoffe²⁸ indicates that, beyond a critical speed, the direction of maximal stress shifts from the propagation direction. This calculation was thought to explain crack branching;²⁹ however, the predicted critical crack speed of 620 m/s in PMMA is well above the critical velocity that we observe.

The observed instability may be only the first of a sequence of instabilities that perhaps culminate in crack branching, as observed in highly stressed brittle materials. Obviously, much work needs to be done to develop a theory to describe this sequence, but our observations indicate that even in the initial regime of crack propagation, before the onset of the instability, current theory does not describe the behavior of the system (see Fig. 7). Our observations should serve as a guide in the development of a theoretical framework.

ACKNOWLEDGMENTS

This work was supported in part by a grant from the Department of Energy Office of Basic Energy Sciences. M. Marder is supported in part by the Sloan Foundation, and J. Fineberg by IBM.

¹A brief account of our work can be found in J. Fineberg, S. P. Gross, M. Marder, and H. L. Swinney, *Phys. Rev. Lett.* **67**, 457 (1991).

²A. K. Green and P. L. Pratt, *Eng. Fract. Mech.* **6**, 71 (1974); W. Doll, *J. Mater. Sci.* **10**, 935 (1975).

³J. M. Huntley, *Proc. R. Soc. London A* **430**, 525 (1990); J. A. Greenwood and K. L. Johnson, *Philos. Mag. A* **43**, 697 (1981); R. M. Christensen and E. M. Wu, *Eng. Fract. Mech.* **14**, 215 (1981); R. A. Schapery, *Int. J. Fract.* **11**, 369 (1975); H. K. Mueller and W. G. Knauss, *Trans. Soc. Rheol.* **15**, 217 (1971); X. Liu and M. Marder (unpublished).

⁴J. D. Eshelby, *J. Mech. Phys. Solids* **17**, 177 (1969).

⁵B. V. Kostrov, *Appl. Math. Mech.* **38**, 511 (1974).

⁶L. B. Freund, *J. Mech. Phys. Solids* **20**, 129 (1972); **20**, 141 (1972); **21**, 47 (1973); **22**, 137 (1974).

⁷X. Liu and M. Marder, *J. Mech. Phys. Solids* **39**, 947 (1991).

⁸M. Marder, *Phys. Rev. Lett.* **66**, 2484 (1991).

⁹Lord Rayleigh, *Proc. London Math. Soc.* **17**, 4 (1885).

¹⁰K. Ravi-Chandar and W. G. Knauss, *Int. J. Fract.* **26**, 141 (1984).

¹¹H. Bergkvist, *Eng. Fract. Mech.* **6**, 621 (1974).

¹²The fracture energy, instead of being a material constant, is assumed to depend on the crack velocity. If one then assumes the behavior of the crack is described entirely by the equations of motion based on linear elasticity, the effective velocity dependence of the fracture energy can be derived.

¹³M. F. Kanninen and C. Popelar, *Advanced Fracture Mechanics* (Oxford University Press, New York, 1985).

¹⁴M. Barber, J. Donely, and J. S. Langer, *Phys. Rev. A* **40**, 366 (1989).

¹⁵J. J. Mecholsky, in *Strength of Inorganic Glass*, edited by C. R. Kurkjian (Plenum, New York, 1985).

¹⁶The exact spacing between the ribs was found to be a function of its molecular weight: R. P. Kusy and D. T. Turner, *Polymer* **18**, 391 (1977).

¹⁷One might argue that the resistance method for determining

the crack length that we use could be unreliable because of either electrical discharge occurring across the crack or because of a variation in the resistance of the aluminum layer due to the stretching of the plate. However, the electrical discharge is not a concern here because the maximum voltage across the entire plate is less than 200 mV in our experiments. Even if this entire voltage drop occurred just across the crack, to obtain the critical electric field of 10 000 V/cm needed for discharge, the crack separation would have to be on the order of 0.1 μm or less. Since the process zone (or the radius of the crack tip) is an order of magnitude larger than this value, discharge is not a concern. The change in the plate resistance due to stretching of the aluminum layer would be given by the change in the cross-sectional area, $\delta A/A$, of the plate due to the applied strain. This can be estimated by $\delta A/A = \sigma E/F \sim 6 \times 10^{-4}$, where σ , E , and F are the Poisson ratio, Young's modulus, and typical applied stress, respectively. The maximal error resulting from this effect would result in a constant shift of less than 0.1 mm in the measured length of the crack. Thus this effect has a negligible effect on our results.

¹⁸Ultrasonic modulation has comparable accuracy, but is intrusive, masking precisely the effects we have observed. See F. Kerkhof, in *Dynamic Crack Propagation*, edited by G. Sih (Leyden, Crows Nest, Australia, 1973), p. 3.

¹⁹This is strictly true when PMMA from the same manufacturer is used.

²⁰W. Doll and G. W. Weidmann, *J. Mater. Sci.* **11**, 2348 (1976).

²¹The craze zone has a maximum dimension of about 50 μm . See W. Doll, L. Konczol, and M. G. Schinker, *Polymer* **24**, 1213 (1983).

²²At V_c the observed oscillations in the velocity signal become consistently larger than our measurement error. However, on the basis of these measurements alone, we cannot rule out the existence of coherent velocity oscillations on the order of our resolution at velocities lower than V_c . Although some fluctuations are seen preceding this point, the Fourier spectrum of the velocity fluctuations shows no evidence of coherent structure before V_c . Also, profilometer measurements of this

region indicate no structure.

²³L. B. Freund, *Dynamic Fracture Mechanics* (Cambridge University Press, New York, 1990).

²⁴The reflected transverse waves arrive from the vertical boundaries when the crack length is $16l_0$ and from the far horizontal boundary after the crack traverses $21.7l_0$ for the lower curve in Fig. 7; the corresponding lengths for the upper crack are $16l_0$ and $20.1l_0$. The reflected longitudinal waves arrive from the vertical boundaries when the crack length is $7.0l_0$ and from the far horizontal boundary after the crack traverses $11.1l_0$ for the lower curve and $7.7l_0$ and $11.5l_0$ for the upper curve. Here the initial crack length l_0 is 5.3 mm for the lower curve and 6.5 mm for the upper curve. The reflections from the near horizontal boundary arrive within the first 1 mm of propagation.

²⁵K. Takahasi, K. Matsushige, and Y. Sakurada, *J. Mater. Sci.* **19**, 4026 (1984).

²⁶The value of V_c determined in this way was not sensitive to the threshold value chosen for $P(x_0)$. For example, the criterion $P(x) > 5P(0)$ for the onset of the instability changes the value of V_c by less than our velocity resolution.

²⁷J. Guckenheimer and P. Holmes, *Nonlinear Oscillations, Dynamical Systems and Bifurcations of Vector Fields* (Springer-Verlag, New York, 1983).

²⁸E. H. Yoffe, *Philos. Mag.* **42**, 739 (1951).

²⁹B. Cotterell, *Appl. Mater. Res.* **4**, 227 (1965); K. Ravichandar and W. G. Knauss, *Int. J. Frac.* **26**, 189 (1984).

³⁰Although the surface amplitudes are measured as a function of crack length, they can be converted to time by using the crack length versus time data obtained for the velocity measurements. The crack length versus time data used in the conversion were time averaged in order to cancel their own oscillatory component.

³¹We obtained the value of the Poisson ratio σ for the PMMA used, by direct measurements of the longitudinal sound velocity in bulk, $c_1 = (E/\rho)^{1/2} \{ (1-\sigma) / [(1+\sigma)(1-2\sigma)] \}^{1/2}$, ($c_1 = 2760$ m/s), where the density ρ and Young's modulus E were measured independently.

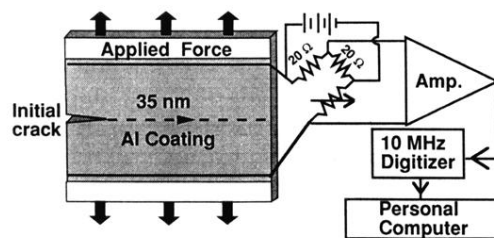


FIG. 2. This schematic representation of the experimental apparatus indicates how resistance measurements are performed to determine the location and velocity of a crack tip. The dashed line indicates the path of the crack.

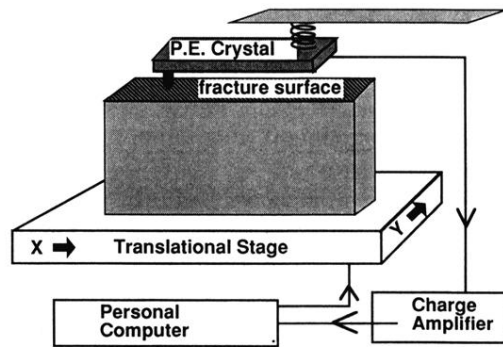


FIG. 3. Schematic diagram of the profilometer used to determine the surface profile of a crack surface. A piezoelectric crystal (P.E.) was used as its sensor.

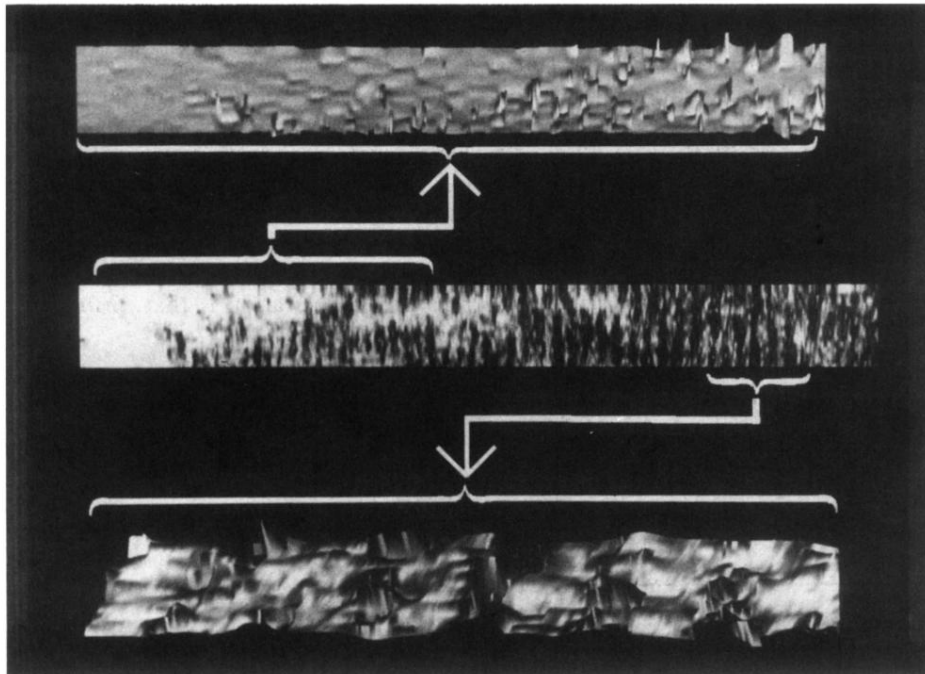


FIG. 4. Computer visualizations of the profilometer data for a crack that propagated from left to right. The central image shows an overview of a portion of the fracture surface, $62 \text{ mm} \times 1.5 \text{ mm}$. Lighting models are used, so that the image is nearly identical to illuminated photographs of the surface. Note the ripple pattern with wavelength on the order of 1 mm . Two subregions have been magnified and shown in perspective. The onset of the instability appears in the upper image; the highest peaks are about $20 \mu\text{m}$. The lower image contains a magnified view of the ripples created by the instability once it develops more fully; the highest peaks are about $50 \mu\text{m}$.